Modelling of Seawater Intrusion in the Magdalen Islands (Québec, Canada)

Jean-Christophe Comte and Olivier Banton

Abstract Magdalen Islands are typical examples of insular regions completely dependent on groundwater everywhere vulnerable to seawater intrusion. To preserve sustainability and quality of the resources, mathematical modelling of the equilibrium between freshwater and marine saltwater appears like a powerful tool of management. However, model quality mainly depends on the previous characterization of the hydrogeological environment. For this purpose, Electrical Resistivity Tomography (ERT) constitutes a relevant geophysical method.

ERT profilings have been carried out on the whole archipelago, with a more densely cover near the main pumping wells. Measured geophysical data has been interpreted by inverse geoelectrical modelling. A variable density flow and transport mathematical model has been first developed using both hydrogeological and inverted geophysical data, and secondly compared, validated and calibrated on coupling forward and inverse geophysical results. Geophysical/hydrogeological comparisons have been facilitated by the establishment of empirical correlation between bulk electrical resistivities (geoelectrical model results) and pore water chloride concentrations (variable density model results). The use of this cross validated hydrogeological model allowed reconstituting the main features of the interface and seawater intrusions imaged by geophysics in the practical case of two high rate pumping wells.

Obtained results display the relevancy of using together resistivity imaging and hydrogeological modelling. Each method allows both validation and interpretation of results obtained by the other method. With such a cross validation, different pumping scenarios can be tested and bring to the elaboration of a sustainable management of groundwater in terms of applied pumping rates and withdrawals spatial distribution.

Index Terms Canada, Electrical Resistivity Tomography, Forward and Inverse Geoelectrical Modelling, Hydrogeology, Magdalen Islands, Seawater Intrusion, Variable density Flow and Transport Modelling

Manuscript received September 2006
This work was supported in part by HYDRIAD (Saint-Bauzély, France), the Laboratory of Hydrogeology of the University of Avignon - LHA, (Avignon, France), the French National Comity of Geology CNFG (Paris, France), the Municipality of The Magdalen Islands (Cap-aux-Meules, Québec, Canada) and the Quebec Fund for Sustainable Development FAQDD (Québec, Québec, Canada).

J. C. Comte is with HYDRIAD, route de Saint-Geniès, 30730 Saint-Bauzély, France, and the Laboratory of Hydrogeology, University of Avignon, 33 rue Louis Pasteur, 84000 Avignon, France (corresponding author phone: +33-(0)6-87-16-10-28; fax: +33-(0)4-66-02-44-45; e-mail: comte@hydriad.com).

O. Banton is with the Laboratory of Hydrogeology, University of Avignon, 33 rue Louis Pasteur, 84000 Avignon, France (e-mail: olivier.banton@univ-avignon.fr).

I. INTRODUCTION

FREQUENT occurrences of saltwater intrusion are found in coastal regions where overexploitation of groundwater causes the encroachment of seawater into freshwater aquifers. Such intrusions allow the degradation of the resources and the slow movement of groundwater makes the remediation time long. For investigation of seawater intrusion, the electrical resistivity geophysical method, which introduces electrical current into the ground through electrodes driven into soil, is effective because the presence of salt increases the bulk electrical conductivity of the soil. The use of such field surveys can reveal the present state of saline interface position and/or seawater intrusion [1]. It, however, cannot make prediction into its evolution and cannot be used for scenario building based on different levels of human activities. Mathematical models are needed for these purposes.

In the last ten years, numerous experiments have coupled electrical geophysics and groundwater transport modelling [2]-[3]-[4]-[5]-[6]-[7]. Most of these works focused on experimental tracing tests, among it a few involving tracer density effect [3]-[5]-[6]. Bates and Robinson [8]-[9] are ones of the few teams coupling geoelectrical surveys to coastal groundwater modelling and management.The present paper exposes an application of the resistivity tomography to assist the modelling of seawater intrusion. The Magdalen Islands (Québec, Canada), located in the Saint-Lawrence Gulf, are totally dependent on groundwater. Some seawater intrusions have been observed in the past and different corrective measures were applied with regards to the reduction of pumping rates [10]. The main objective of the study was to put recommendations on the optimal pumping rates to be applied on actual wells and on the location of new wells.

II. HYDROGEOLOGICAL SETTING

A. Geology

The Magdalen Islands belongs to the Maritimes Permo-Carboniferous Basin included in the North-eastern Appalachian Geological Province [11]. Geology is composed of Carboniferous and Permian Inf. mostly sedimentary rocks deposited in a post-orogenic (Devonian Acadian Orogeny) pre-land basin [12]. The layers thus formed represent deposits stemming from the erosion of mountain chains. Only the

Mississippian marine invasion(s) of Windsor Group is present throughout the continental clastic sequence and mainly comprised of limestone, sandstone, gypsum, anhydrite and salt. Into these continental and shallow marine levels, volcanic and volcano-clastic rocks are frequently interstratified. Permian Inf. dated Grindstone Group overlying the Mississippian Windsor Group is essentially characterized by a fluvio-marine clastic sedimentation of sandstones, siltstones and mudstones that let place to eolian bad-consolidated sandstones and siltstones in the upper levels. Locally disseminated on the archipelago, Quaternary glaciations deposited superficial fluvio-glacial materials filling localized paleo-channels incising Grindstone Group rocks.

Feature structural targets of Magdalen Islands are mostly halokinesis structures as salt dome and pillow. Diapir-related tectonics generated large-scale graben and horst structures and important intra-formational deformations into the volcano-clastic upper Windsor Group ("cap-rock"-type structures, [13]). The horsts (constituting most of the summits of islands) are composed by the Mississippian rocks, while Permian sandstones compose the outcrops in the graben sectors (Fig. 1).

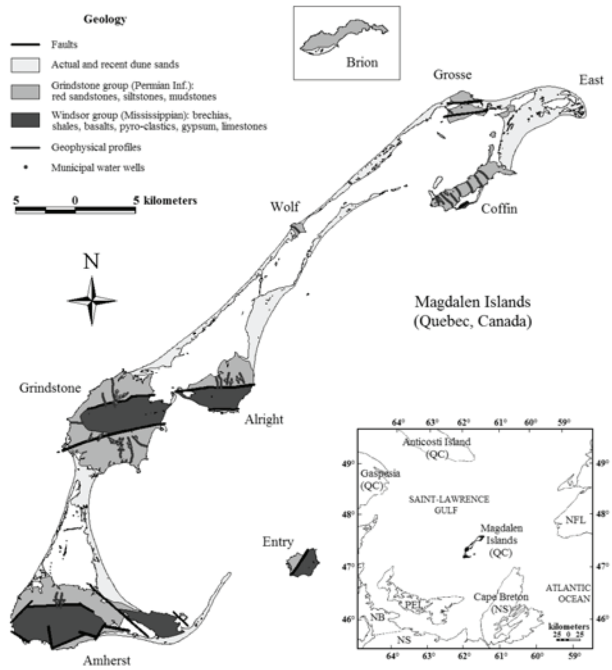

Fig. 1. Simplified geological map of Magdalen Islands archipelago with layouts of geophysical profiles, water wells positions and global location in the east Canadian Maritime region, (NB: New Brunswick; NFL: Newfoundland; NS: Nova Scotia; PEI: Prince Edward Island; QC: Québec).

A. Hydrogeology

Into the Magdalen Islands, Permian sandstone formations (Grindstone Group) constitute the main aquifers while Mississippian horsts (Windsor Group) can be considered as their impervious lateral limits (Fig. 1). With a mean transmissivity of about 4.10^{-3} m^2/s [10] and a mean annual recharge around 230 mm [14], these formations can support very high pumping rate with no consideration for the water quality (i.e. for seawater intrusion). However the bad distribution of both the population and the water wells through the islands generates an unequal pressure of water withdrawals. This bad-distributed pressure has conduced to seawater intrusions.

III. Electrical Resistivity Tomography Surveys

A. ERT method

The Electrical Resistivity Tomography (ERT, also called Direct Current -DC- Resistivity Imaging) is a technique allowing a continuous characterization of the subsurface electrical resistivity [15]-[16]. This geophysical method is widely used for environmental, and especially hydrogeological, applications [16]-[17]-[18].

B. Data Acquisition

Thirty-six (36) 2D resistivity profiles were carried out through the Magdalen Islands using an ABEM Lund System with a 5 m electrode spacing (maximum AB spacing of 360 m). Section lengths vary between 0.4 and 2.3 km, for a cumulative length of 37.6 km (Fig. 1). Measurements were done using the Wenner-Alpha array. ERT results were interpreted using the RES2DINV inverse modelling software (ver. 3.55, [19]) and RES2DMOD forward modelling software (ver. 3.01, [20]).

IV. Geoelectrical Modelling

A. Inverse Modelling

The aim of geoelectrical inverse modelling is to automatically determine, through a computer program (RES2DINV), a two-dimensional (2D) resistivity model of the sub-surface for the data obtained from electrical imaging surveys [21]. Basically, a mathematical optimization method [22]-[23] tries to reduce the difference between the calculated and measured apparent resistivity values by adjusting the resistivity of the model blocks. For seawater intrusion problems in the Magdalen Islands, the robust inversion mode, based on the absolute difference, has been used. It might be more suitable for geological context with homogenously areas separated by a sharp contact, especially for freshwater/saltwater interface imaging.

B. Forward Modelling

Geoelectrical forward modelling is used to reconstitute the resistivity model whose geoelectrical effect correspond to the surface measured (apparent) resistivity data, drawn in a pseudosection. RES2DMOD is a 2D forward modelling program that calculates the apparent resistivity pseudosection for a defined 2D subsurface model. Some improvements were made to the Dey and Morrison [24] finite-difference formulation to improve the accuracy of the calculated apparent resistivity values [25]. In our work, the presented 2D resistivity model totalizes 5800 rectangular cells (29 lines x 200 columns), from surface to 160 m depth. Applied resistivities were calibrated on the measured apparent resistivity pseudosection.

V. Hydrogeological Modelling of Seawater Intrusion on Grindstone Island

A. 3D Density dependent Flow Numerical Modelling

Simulating freshwater/saltwater dynamic equilibrium in a coastal aquifer necessitates numerical code that couples flow equation and transport equation resolution, taking into account density effects related to high concentrations in salt. For this purpose, in application to the Grindstone Island coastal aquifer, the finite-element numerical code SUTRA [26] has been used (SUTRA ver. 2D3D.1, [27]).

B. Location and Hydrogeologic Structure of 3D Model Region

Among the Magdalen Islands, Grindstone Island is the largest and the most populated one. It is also the one having the highest groundwater withdrawals and the largest number of municipal wells. The region modelled covers the south-eastern part of Grindstone Island representing an area of about 6.3 km^2 where outcrop red eolian sandstones (Fig. 2). It extends north from the Mississippian horst contact to south and south-east into the Plaisance Bay, few ten meters behind the coastline, covering the 10 main municipal water wells of Cap-aux-Meules. The inferior limit of the 3D block has been taken to 500 m below sea level in the aim of taking into account the deepest levels of the saline interface according to the local application of the Ghyben-Herzberg's Principle [28]-[29].

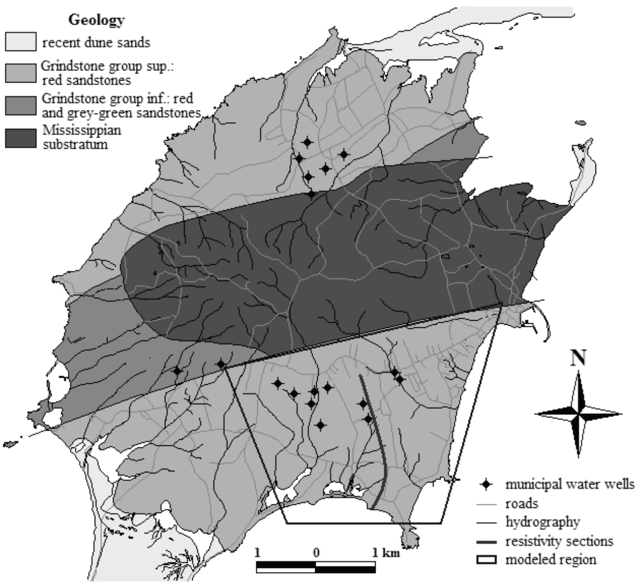

Fig. 2. Geological map of Grindstone Island with location of modelled region and layout of the selected resistivity profile correlated with modeling (Fig. 8).

C. Hydrogeological Parameters and Boundary Conditions

Hydrogeological properties of the aquifer are defined in conformity with the known surface geology of this sector of Grindstone Island (Table I). Four types of boundary conditions were applied on the 3D model: pressure conditions (seawater edges and seafloor), surface flow condition (freshwater recharge), linear flow condition (freshwater lateral supplies), and nodal flow conditions (water wells withdrawals). After historical observations of Sylvestre [30], Sylvestre and Boucher [31] and Madelin'Eau [10], four withdrawal periods have been applied to model: 1966-1975, 1975-1985, 1985-1993, and 1993-2003. Before year 1966 groundwater consumption were carried out with individual low rate water wells, without industrial withdrawals (e.g. fish factories).

VI. Hydrogeoelectrical Portrait of The Magdalen Islands and Freshwater/Seawater Transition Zone Imaging

A. Geological Structures

Fig. 3 shows some typical inverted resistivity sections obtained on Magdalen Islands. The Alright Island section (Fig. 3, top), from horst to coast, reveals the typical stair-type faulted geological structure of Magdalen Island close to the Mississippian horsts: the impervious Mississippian cap-rocks (resistivities up to 100 ohm m), the Grindstone Group inf. compact sandstones (values of about 60 to 100 ohm.m), and Grindstone Group sup. bad-consolidated sandstones (values down to 60 ohm.m). Aplomb the lagoon coastline, the first levels of the mixing zone between freshwater and seawater can be distinguished (resistivities down to 40 ohm m). Freshwater-filled aquifer resistivities can be considered to be comprised between 40 and 100 ohm m (Grindstone Group inf. and sup.).

B. Saline Interface and superficial formations

The Coffin Island section (Fig. 3, bottom), from coast to coast, shows the natural lens shape of the freshwater body (40 to 100 ohm.m) upon seawater (down to 10 ohm.m) separated by a transition zone. The south-eastern slope of the island exhibits high resistivities (up to 150 ohm.m) that indicate the presence of a sand-filled paleo-valley (Quaternary peri-glacial sands) incising Permian eolian sandstones.

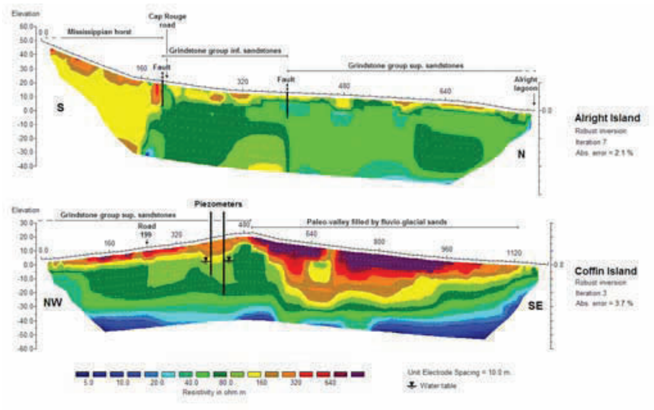

Fig. 3. Two typical inverse model resistivity profiles of Magdalen Islands

few meters downstream the coastal line (Fig. 4). Water wells are responsible to significant drawdowns, especially important for W1, W2 and W3 that presents the highest pumping rates and the lowest distance to coast. Flow velocities display mean values of about 100 m/y (40 to 150 m/y) on the whole domain. Simulated heads of year 2003 reproduce with satisfaction April 2003 observed heads in the close vicinity of wells. Logically, simulations based on mean annual recharge and pumping rates are slightly lower than high-waters April observations.

TABLE I
PARAMETERS AND BOUNDARY CONDITIONS APPLIED TO THE MODEL

Parameter	Units	Value(s)			
Model boundary conditions					
Surface model recharge	(mm/y)	230			
Subsurface entering lateral flows	(L/s)	30			
Combined pumping rates	(L/s)	16 to 55 depending on the period			
Conductance of seawater pressure boundary	(L.s)	0.00007			
Aquifer hydrogeological properties		Layer 1: Grindstone Group sup. (25 to -25 m)	Layer 2: Grindstone Group sup. (-25 to -50 m)	Layer 3: Grindstone Group inf. (-50 to -75 m)	Layer 4: Grindstone Group inf. (-75 to -500 m)
Isotropic permeability	(m^2)	$1.25\ 10^{11}$	$2.65\ 10^{12}$	$6.1\ 10^{13}$	$1.4\ 10^{13}$
Specific yield of water table layer	(%)	16	-	-	-
Effective porosity	(%)	5	2	0.8	0.3
Isotropic longitudinal dispersivity	(m)	30	30	40	40
Isotropic transverse dispersivity	(m)	1.5	1.5	2	2

VII. 3D Simulations of Grindstone Island Aquifer and Effects of Pumping Rates on Freshwater/Seawater Transition Zone

A. Simulation Modes

Hydrodynamic simulations of Grindstone coastal aquifer were obtained by application of transient-state simulation modes. An initial hydrogeological steady-state without well withdrawals has been simulated in order to represent pre-1966 period. Before 1966, freshwater/seawater transition zone is assumed to be equilibrated with a low and diffuse individual groundwater consumption. Then the four successive pumping rate transient periods has been simulated until year 2003. Pumping rates are constant into each of these periods. Model results of year 2003 are extracted for comparison to 2003 field data.

B. Calculated Groundwater Water Table and Flow Velocities

Groundwater flows from horst contact to the seashore in a general NW to SE direction, from a maximum head of 8 m above sea level in the NW corner of the model to sea level

C. 3D Modelling of Seawater Intrusions

3D salt concentration distributions of year 2003, resulting from groundwater pumping since 1966, have been extracted from model (Fig. 5). Freshwater appears as a floating-lens upon saltwater that enters aquifer from the seafloor.

Mixing zone between freshwater and seawater corresponds to a transition zone with metric to decametric width. Average depth of transition zone middle surface is consistent with static freshwater/seawater interface predicted by Ghyben-Herzberg's law in regard with simulated water table. Seawater upcoming spots can be observed under most of simulated water wells, especially those implanted the nearest from the sea (WU9, WU10, W1, W2 and W3). As observed, for these five wells, pumped water presents higher salinities than freshwater (50 to 1'200 mg/L chloride), without nevertheless reach those of St-Lawrence Gulf seawater (about 15'700 mg/L chloride).

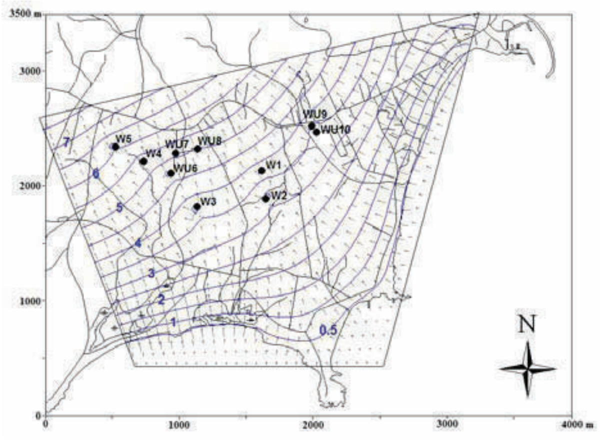

Fig. 4. Year 2003 simulated water table elevation (blue contour lines, in m above sea level) and velocity vectors (projected to horizontal) at 2.5 m under sea level

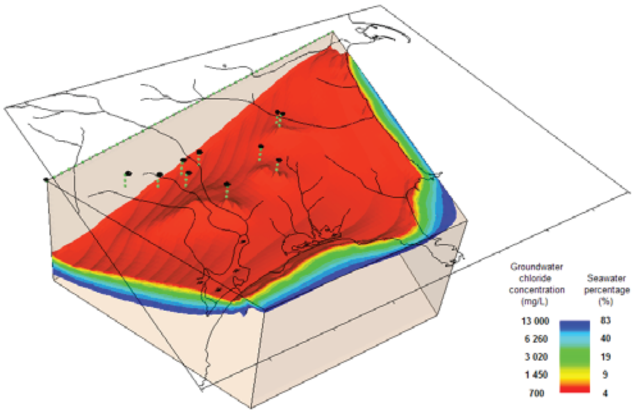

Fig. 5. 3D simulation of the freshwater/saltwater transition zone and saltwater intrusion spots in modelled region of Grindstone Island (vertical exaggeration is three times).

VIII. Cross-Validation between Forward/Inverse Geoelectrical Modelling and Variable-density Flow Modelling

A. Relation between Bulk Electrical Resistivity and Pore Water Chloride Concentration on the Magdalen Islands

To correlate geophysical surveys results with model simulations a relation between bulk electrical resistivity and pore water chloride concentration must be established. This relation has been decomposed in four empirical equations: (1) bulk electrical resistivity as a function of pore water resistivity (Archie's Law, [32]); (2) electrical conductivity as a function of temperature [33]; (3) pore water conductivity as a function of total dissolved solids contents (TDS, regional physico-chemical data, Fig. 6); and (4) TDS as a function of chloride concentration (regional chemical data; Fig. 7).

B. Comparison between Inverse/Forward Geoelectrical and Variable density Flow Modelling Results

Fig. 8 illustrates the comparison between ERT inverse model section (Fig. 8, 2nd section from top), ERT forward model section (Fig. 8, 3rd section) and hydrogeological model sections (Fig. 8, 4th and 5th sections) near wells W1 and W2 in the centre of the modelled region. First section on Fig. 8 illustrates measured geoelectrical data pseudosection on which inverse and forward resistivity models are calibrated. Variable-density model sections compares known actual and twice known actual pumping rates. The two wells were drilled in 1993 and operated since this date.

In the saturated zone, geophysical inverted results show conductivity gradients increasing with depth corresponding to an increasing salinity from down to 50 mg/L chloride (freshwater) to up to 3'000 mg/L (saline water imaged in the south bottom section corner). Direct downstream well W2 a dissymmetric saline upward spot is observable, while analogous anomaly is more difficult to be clearly distinguished near W1.

Forward model resistivity section shows three zones of salinity increasing with depth: the freshwater saturated sandstones with resistivity of 100 ohm m, the seawater saturated sandstones with resistivity of 2 ohm m and the transition zone of about 50 ohm.m. Although upcoming spot are also identifiable under the two wells, transition zone appears at lower depths than transition levels calculated by the inverse model. This is due to the deepest levels taking into account in the forward model (until 160 m depth with very low applied resistivities). Also, forward modelled freshwater lens discharges up to 200 m behind the seashore, information that inverse model section, which is limited to the measured pseudosection window, cannot provide.

Hydrogeological modelling reproduces this upcoming phenomenon. Both cases of applied pumping rates generate a high salinity gradient under well W2 due to an upcoming vertical saline spot. An oblique spot also appears downstream W1, but reaches the geophysical observation window only in the case of the application of doubled pumping rates. Furthermore, results of single pumping rates model are very close to the results of forward geophysical model although effect of twice rates approaches this of inverse geophysical model.

Finally, main differences between geophysics and variable-density model concerns sections smoothing. While hydrogeological and forward geophysical modelled transition zone appears smoothed, inverse geophysical section shows many horizontal oscillations that can be related to the depth propagation of surface heterogeneities. Also, contrary to the hydrogeological modelled state, observed geophysical state is an instantaneous record of transient flow and pumping conditions which can be responsible of spatial oscillations of the transition zone and obliquity of the upcoming spots.

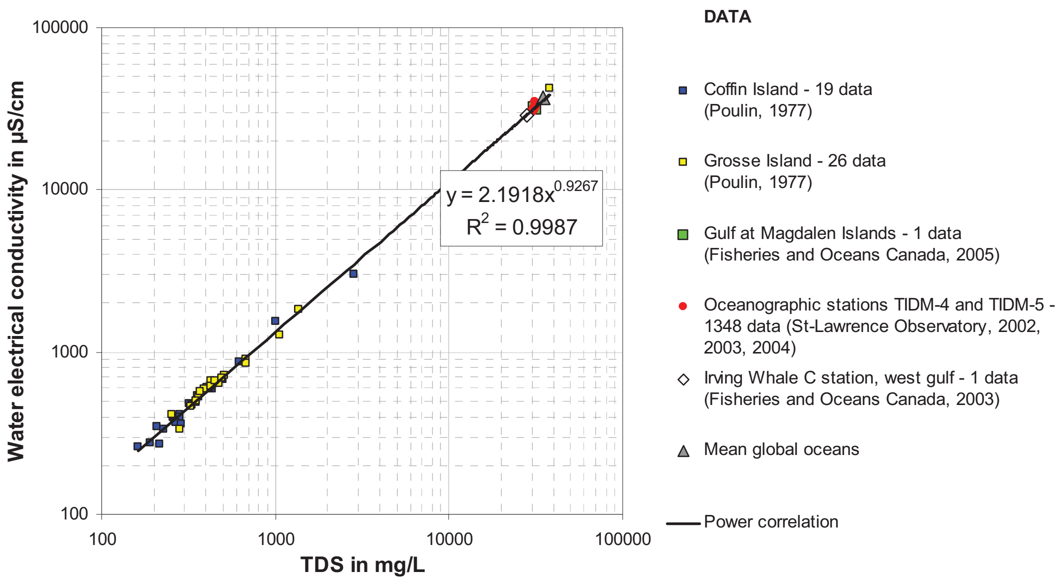

Fig. 6. Correlation between total dissolved solids (TDS) and electrical conductivity in Magdalen Islands' groundwater and seawater.

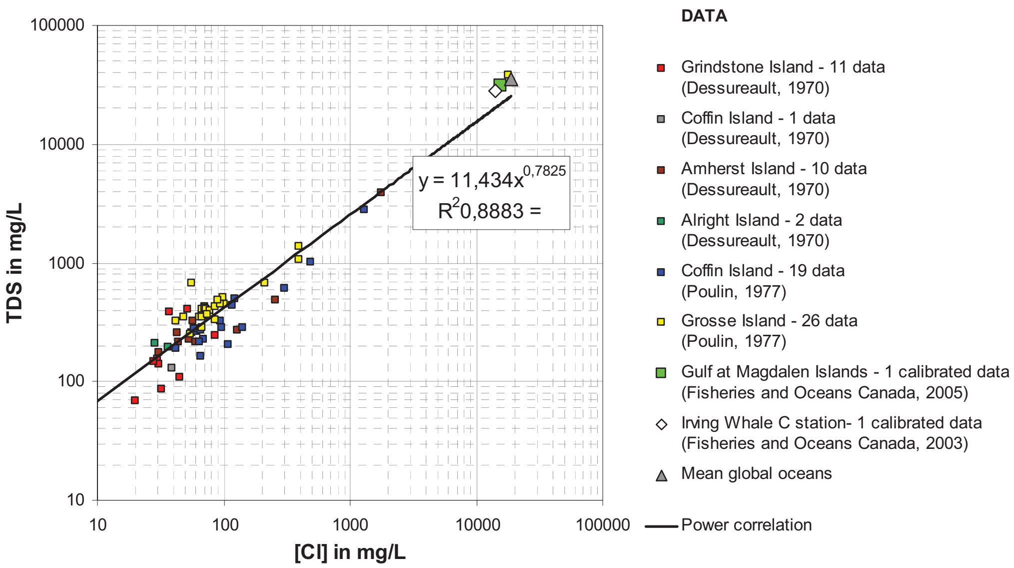

Fig. 7. Correlation between chloride concentrations and total dissolved solids (TDS) in Magdalen Islands' groundwater and seawater

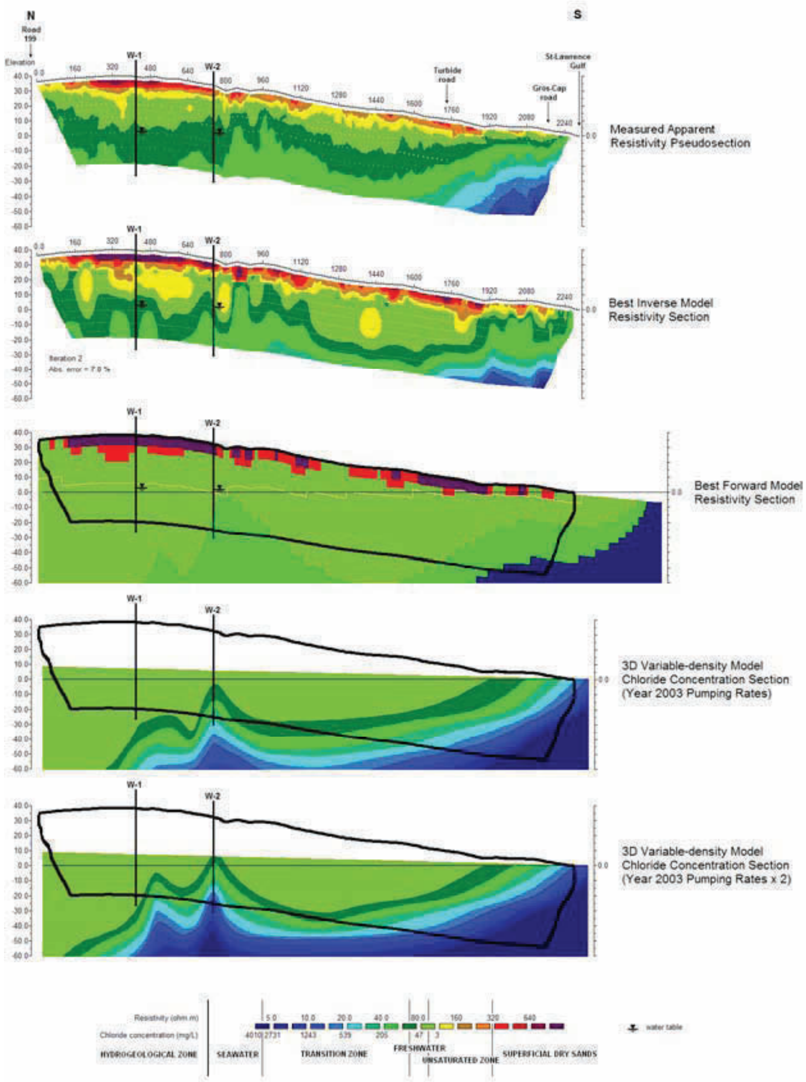

Fig. 8. Comparison between geophysical sections (3 Fig. on top, resistivity in ohm.m) and variable-density flow model sections (2 Fig. on bottom, chloride concentration in mg/L) of saltwater intrusion in the centre of modelled region (wells W-1 and W-2).

C. *Discussion about Pumping Rates*

Concerning the two withdrawal cases applied to the model, doubled pumping rate approaches the one used during the summer period where both the population and the consumption significantly increase in the Magdalen Islands. Results on the bottom section then would correspond to the application all the time over the year of the summer pumping rates. Obviously, seawater intrusions and transition zone upcoming appear higher for doubled pumping rates than for mean annual rates. For more increasing withdrawals, water quality on wells W1 and W2 would be seriously compromised with significant salt concentrations. In actual situation, however, the summer pumping rates do not induce serious contamination because of the short duration of this regime during only few months. These observations also concerns Grindstone wells that are not considered in theses geophysical/hydrogeological modelling comparisons.

IX. CONCLUSIONS

The joint application of variable-density flow and transport modelling and electrical resistivity tomography conduced to characterize groundwater behavior with relation to seawater intrusion into the aquifer. Coupling geophysical inverse and forward modelling results facilitated the physical 3D construction, calibration and validation of the hydrogeological variable-density model by providing relevant information on geological structure and distribution of salt concentrations

through the coastal aquifer. As a return, hydrogeological modelling allowed fine interpretation, discussion and validation of geophysical results, in particular the distinction between resistivity anomalies that can be explained by the intrusion modeled phenomenon and those for which another cause or origin must be invocated. Each method produces results whose crossing allows more advanced hydrogeologic understanding and interpretations than simple addition of each tool independently considered.

Geophysical/hydrogeological "cross-validated" results show that the actual water wells withdrawals induce significant upcoming of freshwater/seawater transition zone into the coastal aquifer and local intrusion spots under some wells.

Comparisons between two modelled pumping cases and geophysical imaging also revels that observed effects of pumping rates on transition zone in Grindstone Island correspond to a compromise between application of actual mean annual pumping rates and doubled ones. Moreover, if the pumping rates are increased, i.e. if the summer pumping rates would be maintained over the year, a high degradation of the water quality would be generated.

Regional-scale seawater intrusion modelling shows that the transition zone upcoming and intrusion spots mainly take place just downstream the wells that are downstream another well. This confirms that the optimal spatial distribution of wells is a lateral implantation perpendicular to the flow direction.

ACKNOWLEDGMENT

Authors thank consortium partners and collaborators: Denis Richard (Agéos Inc., Montréal, Québec, Canada), Renald McCormack (Envir'Eau Puits Inc., Québec, Québec, Canada), and Jean-François Moreau (Saint-Brieuc, France).

REFERENCES

[1] S. R. Wilson, M. Ingham, and J. A. McConchie, "The applicability of earth resistivity methods for saline interface definition," *J. Hydrology*, vol. 316, pp. 301 312, 2006.

[2] M. Morris, "Geoelectrical monitoring of a tracer injection experiment: modelling and interpretation," *Eur. J. Environ. Eng. Geophys*., vol. 1, pp. 15 34, 1996.

[3] L. Slater, A. Binley, and W. D. D. R. Johnson, "Cross-hole electrical imaging of a controlled saline tracer injection," *J. Appl. Geophys*., vol. 44, pp. 85 102, 2000.

[4] A. Kemna, J. Vanderborght, B. Kulessa, and H. Vereecken, "Imaging and characterisation of subsurface solute transport using electrical resistivity tomography (ERT) and equivalent transport models," *J. Hydrology*, vol. 267, pp. 125 146, 2002.

[5] L. Slater, A. Binley, R. Versteeg, G. Cassiani, R. Birken, and S. Sandberg, "A 3D ERT study of solute transport in a large experimental tank," *J. Appl. Geophys.*, vol. 49, pp. 211 229, 2002.

[6] M. Beinhorn, P. Dietrich, and O. Kolditz, "3-D numerical evaluation of density effects on tracer tests," *J. Contaminant Hydrology*, vol. 81, pp. 89 105, 2005.

[7] J. Vanderborght, A. Kemna, H. Hardelauf, and H. Vereecken, "Potential of electrical resistivity tomography to infer aquifer transport characteristics from tracer studies: A synthetic case study," *Water Resour. Res.*, vol. 41, pp. 23, 2005.

[8] C. R. Bates and R. J. A. Robinson, "Geophysics and groundwater modelling of coastal golf courses," *Golf Research News*, vol. 1, n.3, pp. 2-10, 2000.

[9] C. R. Bates and R. J. A. Robinson, "Geophysical surveys for groundwater modelling of coastal golf courses", in *62nd EAGE Conference and Technical Exhibition*, Glasgow, Scotland, 29 May 2 June, 2000, pp. 1-5.

[10] Madelin'Eau, "Gestion des eaux souterraines aux Îles-de-la-Madeleine, Un défi de développement durable, Méthodologie de l'étude," Rapport final, Doc. 1, 61 p., 2004.

[11] D. Brisebois, "Lithostratigraphie des strates permo-carbonifères de l'archipel des Îles-de-la-Madeleine," Min. de l'Energie et des Ressources, Dir. Gén. des Energies Conventionnelles, Serv. de l'Exploration, Québec, Rep. DPV-796, 1981, 48 p.

[12] N. Hayward, A. Grant, S. A. Dehler, and P. Durling, "Geophysical investigation of salt tectonics and structure in the Eastern Magdalen Basin," in Mining Matters for Nova Scotia 2001, Rep. ME 2001-2, Nova Scotia Natural Resources, Mineral and Energy Branch, p. 20, 2001.

[13] M. R. La Flèche, G. Camiré, and G. A. Jenner, "Geochemistry of post-Acadian, Carboniferous continental intraplate basalts from the Maritimes Basin, Magdalen Islands, Québec, Canada," *Chemical Geology*, vol. 148, pp. 115 136, 1998.

[14] Y. Leblanc, "Analyse et modélisation numérique de huit puits de production sur l'Île du Cap-aux-Meules, Îles-de-la-Madeleine," Essai de maîtrise, Univ. Laval, Québec, Canada, 1994.

[15] T. Dahlin, "On the automation of 2D resistivity surveying for engineering and environmental applications," Ph.D. Thesis, Department of Engineering Geology, Lund University, Sweden, 1993.

[16] T. Dahlin, "The development of DC resistivity imaging techniques," *Computers and Geosciences*, vol. 27, pp. 1019-1029, 2001.

[17] S. S. Hubbard and Y. Rubin, "Introduction to hydrogeophysics," in *Hydrogeophysics*, Y. Rubin and S. S. Hubbard Ed., Springer, New York., 2005, pp. 3 21.

[18] R. J. Owen, O. Gwavava, and P. Gwaze, "Multi-electrode resistivity survey for groundwater exploration in the Harare greenstone belt, Zimbabwe," *Hydrogeology Journal*, vol. 14, pp. 244 252, 2005.

[19] M. H. Loke, "RES2DINV ver. 3.55 for Windows 98/Me/2000/NT/XP, Rapid 2-D Resistivity & IP inversion using the least-squares method," GEOTOMO SOFTWARE, Software manual, 2006.

[20] M. H. Loke, "RES2DMOD ver. 3.01, Rapid 2D resistivity forward modelling using the finite-difference and finite-element methods," Software manual, 2002.

[21] D. H. Griffiths and R.D. Barker, "Two-dimensional resistivity imaging and modelling in areas of complex geology," *J. of Applied Geophysics*, vol. 29, pp. 211-226, 1993.

[22] C. de Groot-Hedlin and S. Constable, "Occam's inversion to generate smooth, two-dimensional models from magnetotelluric data," *Geophysics*, vol. 55, pp. 1613-1624, 1990.

[23] M.H. Loke and R. D. Barker, "Rapid least-squares inversion of apparent resistivity pseudosections by a quasi-Newton method," *Geophysical Prospecting*, vol. 44, pp. 131-152, 1996.

[24] A. Dey and H. F. Morrison, "Resistivity modelling for arbitrary shaped two-dimensional structures," *Geophysical Prospecting*, vol. 27, pp. 1020-1036, 1979.

[25] M. H. Loke, "The inversion of two-dimensional apparent resistivity data," Unpubl. Ph.D. thesis, Univ. of Birmingham, U.K., 1994.

[26] C. I. Voss, "SUTRA: A finite-element simulation model for saturated-unsaturated, fluid-density-dependent ground-water flow with energy transport or chemically reactive single-species solute transport," U.S.G.S. Wat. Res. Investigation Report 84-4369, 1984.

[27] C. I. Voss and A. M. Provost, "SUTRA: A model for saturated-unsaturated variable-density ground-water flow with solute or energy transport," U.S.G.S. Wat. Res. Investigation Report 02-4231, 2002, ver. June 21, 2003.

[28] W. Baydon-Ghyben, "Nota in verband met de voorgenomen putboring nabij Amsterdam," *Koninklyk Instituut Ingenieurs Tijdschrift (The Hague)*, pp. 8-22, 1888 1889.

[29] A. Herzberg, "Die Wasserversorgung einiger Nordseebader," *J. Gasbeleuchtung und Wasserversorgung (München)*, vol. 44, pp. 815-819, pp. 842-844, 1901.

[30] M. Sylvestre, "A finite element model for salt water upconing and its application to the Magdalen Islands aquifer," M.S. thesis, Univ. of Waterloo, Ontario, Canada, 1974.

[31] M. Sylvestre and J. M. Boucher, "Eau potable aux Îles-de-la-Madeleine, Problématique, Situation et propositions," Tech. Rep , 17 p., 1985.

[32] G. E. Archie, "The electrical resistivity log as an aid in determining some reservoir characteristics," *Trans. Am. Inst. Min. Metall. Pet. Eng.*, vol. 146, pp. 54-62, 1942.

[33] J. J. Arps, "The effect of temperature on the density and electrical resistivity of sodium chloride solutions," *Trans. AIME,* vol. 98, pp. 327 328, 1953.